



29 **1 Introduction and Background**

30 There have been numerous studies on observing and understanding the changes in tropospheric
31 ozone both regionally and globally, as described recently in Gaudel et al. (2024). Those
32 investigators use both satellite and balloon data to arrive at their findings. One possible
33 opportunity to obtain early estimates of tropospheric ozone from satellite datasets comes from
34 both the Limb Infrared Monitor of the Stratosphere (LIMS) and the Total Ozone Mapping
35 Spectrometer (TOMS) instruments that operated from onboard the Nimbus 7 satellite. LIMS
36 provided ozone profiles from the middle mesosphere to near the tropopause from October 25,
37 1978, to May 28, 1979, both day and night and with a duty cycle of about 6 days on followed by
38 one day off. TOMS made measurements of ultraviolet (uv) molecular scattered and reflected
39 radiation from the ground or cloud tops during daylight. Total ozone was determined from the
40 TOMS measurements via the method of differential absorption at its uv wavelengths during
41 daylight. TOMS provides good data coverage, although it also lacks observations for one orbit
42 many days. This study reports on estimates of tropospheric column ozone (TRCO) obtained by
43 subtracting LIMS stratospheric column ozone (SCO) from TOMS ozone. Initial estimates of
44 layer ozone based on the LIMS Version 5 (V5), SBUV Version 5 data, and sonde profiles are
45 noted, followed by earlier and current estimates of TRCO based on the archived LIMS Version 6
46 (V6) and TOMS Version 8 datasets.

47

48 Remsberg et al. (1984, their Fig. 15) compared V5 stratospheric ozone with correlative ozone
49 measurements obtained by several independent methods, and they judged the V5 ozone as
50 reasonably accurate, except at and below the 50 or 70-hPa level where ozone was biased high.
51 Their calculations involved integrating a V5 profile from the lower mesosphere to the 50 or 70-
52 hPa level and then adding its sum to column ozone from the ground to those same levels from
53 coincident Brewer-Mast (BM) and Electrochemical Concentration Cell (ECC) sonde profiles.
54 They reported that total ozone obtained in that way agreed with Dobson station measurements to
55 within the combined uncertainties of the respective ozone measuring techniques.

56



57 Remsberg and Wu (1989) compared LIMS V5 ozone with concurrent ozone distributions from
58 the Solar Backscatter Ultraviolet (SBUV) and Stratospheric Aerosol and Gas Experiment
59 (SAGE) satellite instruments. They obtained V5 stratospheric zonal mean ozone in terms of
60 Umkehr layer amounts following a mapping of the V5 profiles. In general, their intercomparison
61 results were also within the combined errors of the several techniques, except again in the
62 lowermost stratosphere where the V5 ozone values were biased high. It was unclear at that time
63 what were the cause(s) of bias(es) in V5 ozone in the lowermost stratosphere, although it was
64 clear that there would be significant biases for calculated TRCO, as a result.

65

66 Fishman and Larsen (1987) made separate determinations of the zonal variations of TRCO by
67 integrating Stratospheric Aerosol and Gas Experiment (SAGE) ozone profiles from 1 to 100 hPa
68 and subtracting their SCO values from coincident TOMS measurements. They reported that the
69 SAGE ozone profiles were accurate throughout the stratosphere for determining SCO and in turn
70 the TRCO. In a more comprehensive study, Fishman et al. (1990) analyzed ozone profiles from
71 the follow-on SAGE II instrument, and they found seasonal changes of TRCO and longitudinal
72 excesses of TRCO at tropical latitudes. They reported indications of the production of ozone
73 downwind of biomass burning regions. Ziemke et al. (1998) developed a convective cloud
74 differential (CCD) algorithm for the determination of tropical TRCO directly from the TOMS
75 data and over a span of many more years. They confirmed the initial conclusions of Fishman et
76 al. (1990) in terms of longitudinal and seasonal increases in tropospheric ozone related to
77 instances of biomass burning.

78

79 Remsberg et al. (2007) reported on a LIMS V6 Level 2 (or profile) ozone dataset using improved
80 algorithms for the registration of the LIMS radiance profiles and improved line parameters for
81 retrievals of both temperature and ozone. Based on those findings, Remsberg et al. (2013) added
82 the V6 profiles to an assimilation model and found reasonable agreement for total ozone from the
83 model analysis versus TOMS V8 ozone. The present study considers the use of the LIMS Level
84 3 (map) product for calculations of SCO and then subtracts that amount from TOMS data to
85 obtain TRCO. Section 2 reviews the quality of the LIMS V6 ozone in the lower stratosphere.
86 Section 3 reports on monthly zonal mean TRCO values based on LIMS and TOMS data. Section



87 4 then shows the distributions of TRCO with longitude and latitude for several representative
88 days of the LIMS V6 and TOMS data in November 1978 and in March and May 1979. Section 5
89 reports that daily V6 estimates of TRCO for November compare well with that of Fishman et al.
90 (1990) and of Ziemke et al. (2006), specifically regarding its elevated ozone downwind of
91 biomass burning regions in West Africa. Section 6 summarizes the findings and the details that
92 are in the *Supplement*.

93

94 **2 Quality of LIMS V6 Ozone in the Lower Stratosphere**

95 Remsberg et al. (2007) compared V6 Level 2 zonal average ozone profiles with those from
96 SBUV Version 8 (V8) for three specific days—8 November 1978, 15 March 1979, and 6 May
97 1979 (see their Figure 8). The V6 profiles have an effective vertical resolution of 3.7 km, not
98 unlike those of SBUV. Figure 1 shows the results for V6 minus SBUV data of McPeters et al.
99 (1984). There is a pattern to the differences in the upper stratosphere that is related to how well
100 each measurement technique resolves the effects of the semi-annual oscillation (SAO) in ozone.
101 V6 ozone is slightly smaller than SBUV ozone at tropical latitudes for levels from 10 to 50 hPa,
102 below which there are only a limited number of V6 profiles, due to a screening for effects of
103 emission/extinction from thin cirrus clouds. On the other hand, V6 ozone is larger than SBUV
104 from 15°S to 40°S latitude all three months and from 15°N to 30°N in March and May between
105 the 30 and 70-hPa levels.

106

107 Even though Remsberg et al. (2007) concluded that V6 ozone was improved over that of V5,
108 estimates of V6 accuracy (from their Table 1) are still no better than 20 to 30% in the lowermost
109 stratosphere. LIMS ozone has a large response at those levels to uncertainties in the associated,
110 retrieved V6 temperatures (± 1.2 K); a temperature bias of -1.2 K leads to an ozone bias of order
111 +20% at 50 and 100 hPa. There are also potential ozone errors of 6% and 15% at 50 and 100
112 hPa, respectively, due to uncertainties in the V6 forward model for ozone.

113



114 The archived V6 ozone profiles include a screening of first-order cloud contamination effects
115 below the 45-hPa level and equatorward of $\pm 30^\circ$ latitude, as based on the changes with altitude
116 for the retrieved ozone mixing ratio profile. That “V6 cloud detection” algorithm checks about
117 the vertical gradient of ozone and assigns a cloud index, when ozone mixing ratio increases with
118 decreasing altitude beyond a threshold amount (see Remsberg et al., 2007). The same detection
119 algorithm was also applied at and below the 100-hPa level at higher latitudes, where there may
120 also be false indications of cloud effects due to a vertical layering of the ozone profiles near the
121 tropopause. Yet, one bias that was not characterized for V6 ozone is the likelihood of residual
122 contamination effects in the tropics to subtropics from thin or subvisible cirrus just above the
123 100-hPa level or near the tropopause. An example of the presence of cirrus is in the *Supplement*.
124 Climatological ozone values have been substituted at 68 hPa ($\pm 12^\circ$ latitude) and at 100 hPa
125 ($\pm 18^\circ$ latitude) for calculations of SCO in the current study to avoid residual cirrus effects.

126

127 To check whether temperature errors are a significant source of bias for SCO, the V6 Level 2
128 temperature profiles are compared with those from MERRA in Figure 2 for one day, 26 January
129 1979, and for the latitude band of 20°S to 20°N . Note that their zonal standard deviations about
130 the respective zonal means agree (top right), an indication that both data sets are equally
131 responsive to zonal temperature waves. Their zonal averages (bottom left) show that the V6
132 temperatures have net positive biases from the middle stratosphere and into the mesosphere, or in
133 a region where temperature tides are present and where the MERRA temperatures are not highly
134 accurate due to the low vertical resolution of its operational stratospheric sounder unit (SSU)
135 radiance data. Even so, a V6 temperature bias at those upper altitudes leads to only small errors
136 in V6 ozone (and SCO). However, there are negative differences of nearly -1 K at about 30 and
137 50 hPa or where ozone partial pressure makes large contributions to SCO. At middle latitudes
138 there are negative temperature differences for this day in the SH but not the NH (see details in
139 the *Supplement*). There are rather large positive differences in Fig. 2 near the tropical
140 tropopause, which leads to retrieved V6 ozone of near zero values at 68 and 100 hPa. But this
141 region is also where the current study substitutes climatological ozone for calculations of tropical
142 SCO to avoid effects of cirrus contamination.

143



144 Temperature bias impacts retrievals of LIMS ozone in two ways. It affects (1) the registration of
145 ozone radiance with pressure or the conversion of the observed radiance versus altitude onto a
146 pressure-altitude grid prior to a retrieval of V6 ozone, and (2) the determination of ozone mixing
147 ratios from the radiances, where the effect of temperature is accounted for via a forward
148 calculation of Blackbody radiance in the ozone channel. Ozone radiance versus altitude profiles
149 were registered in terms of radiance versus pressure both below and above the pressure versus
150 relative altitude reference level of 20 hPa, and the small, net effect of (1) reflects the presence of
151 any temperature biases. On the other hand, the relation of temperature to radiance from (2) is
152 non-linear, such that where temperatures are biased cold (at 30 to 50 hPa) too little of the
153 calculated (forward) radiance is due to temperature. As a result, accounting for the remaining
154 radiance leads to retrieved V6 ozone mixing ratios and associated SCO values that are too large.
155 As described in Remsberg et al. (2021), there are also ascending versus descending orbital
156 differences in retrieved ozone that change sign between the SH and NH in the subtropics to
157 middle latitudes. However, the combined orbital profiles are used for the present analysis.

158

159 **3 Estimates of monthly, zonal mean TRCO**

160 The results of Fig. 1 are also compared using monthly zonal mean TRCO values. TRCO versus
161 latitude is determined by calculating LIMS monthly mean SCO down to near the tropopause and
162 subtracting those values from monthly TOMS total ozone for the months of November 1978
163 through May 1979. The tropopause extends to about the 100-hPa level between $\pm 30^\circ$ latitude
164 most months (Logan, 1999; Ziemke et al., 2006). Monthly LIMS data are from its Version 6
165 (V6) Level 3 product (Remsberg and Lingenfelser, 2010), as provided to the SPARC data
166 initiative (or SPARC DI) (see *zenodo* archive in Hegglin et al., 2021). V6 tropical zonal mean
167 ozone profiles are integrated from 0.7 to 100 hPa to give monthly zonal mean estimates of SCO
168 versus latitude. Monthly TOMS data are from
169 https://data.gesdisc.earthdata.nasa.gov/data/Nimbus7_TOMS_Level3/TOMSN7L3ztoz.008/TO
170 [MSN7L3ztoz_19781101_19930506.tar.gz](https://data.gesdisc.earthdata.nasa.gov/data/Nimbus7_TOMS_Level3/TOMSN7L3ztoz.008/TOMSN7L3ztoz_19781101_19930506.tar.gz).

171



172 Monthly TRCO results versus latitude are in Table 1. TRCO ranges from about 20 to 40 DU at
173 equatorial latitudes, which agrees with TRCO estimates from more recent satellite data (Ziemke
174 et al. 2006). There is a monthly progression toward higher values at 30N that is reflective of the
175 seasonal changes of ozone at that latitude. Results are nearly steady in the tropics. Yet, there is
176 also a progression toward zero and slightly negative TRCO values in the southern subtropics that
177 is clearly unrealistic. It may be that the LIMS SCO values have positive biases in the SH,
178 leading to TRCO values that are trending lower (c.f., Fig. 1). The results for March and May are
179 discussed in the next section.

180

181 Are there any anomalous trends in the TOMS data of 1978-79? Herman et al. (1991) reported
182 that the measured solar flux values from Nimbus 7 TOMS were affected by a degradation of the
183 surface of and reflectivity from its diffusor plate during the first months of its operations.
184 Diffusor plate degradation amounts to a spurious reduction in total column ozone, and they
185 developed corrections for that and applied them to the TOMS V8.6 dataset from January 1979
186 onward. Herman et al. (1991, their Figure 4) also showed that there was a ~4% increase in the
187 measured solar flux at the wavelength of 380 nm from late October 1978 to January 1979 due to
188 the gain in the photomultiplier tube detector. That increase affects the measured reflected fluxes
189 from the surface and cloud tops and translates to a decrease in inferred total ozone. Although
190 they did not do so, a correction for that change would increase TOMS total ozone for January
191 through May (in Table 1) by about 10 DU at all latitudes, not just in the SH subtropics.

192

193 Ziemke et al. (1998) and Ziemke et al. (2006) reported seasonal changes in both total ozone and
194 tropospheric ozone at several SH tropical and subtropical stations. They found that tropical
195 TRCO values decreased generally from about 45 DU in November to 25 DU in May or by about
196 20 DU, and they attributed most of those seasonal changes in total ozone to changes in the
197 tropospheric column. TOMS ozone in 1978/1979 decreased by about 15 DU from 8 November
198 to 6 May at Natal, Brazil. On the other hand, Dobson total ozone at Natal decreased by 35 DU
199 from 19 November 1978 to 5 May 1979. Table 1 shows that the monthly zonal mean TRCO at
200 5°S (near Natal) decreased from 44 DU to 14 DU, or by 30 DU. Making the foregoing upward
201 adjustment of 10 DU in TOMS ozone would lead to the same increase in TRCO and a change of



202 only 20 DU from November to May. Nevertheless, such an adjustment does not account for the
203 rather large decreases in TRCO in Table 1 for the SH subtropics. TOMS/Dobson ozone
204 comparison checks at stations are provided in the next section, at least when Dobson station data
205 are available.

206

207 **4 Distributions of SCO and TRCO from TOMS and LIMS**

208 **a. 15 March 1979**

209 As noted from Fig. 1, V6 ozone has rather large differences with SBUV ozone in the subtropical
210 lowermost stratosphere for both 15 March and for 6 May. What is the nature of TRCO at those
211 latitudes? Figure 3 shows the distribution of total ozone from a subset of daily gridded TOMS
212 Version 8.6 ozone data for 15 March, where the original TOMS grid has a spatial resolution of 1°
213 latitude \times 1.25° longitude and was resampled (but not interpolated or smoothed) to match a $2^\circ \times$
214 5° grid of the corresponding LIMS V6 ozone field. TOMS data are compared with the LIMS
215 ozone from 84°N to 64°S for this study. The vertical white slice (near 20°W) is where TOMS
216 made no observations that day.

217

218 The red dots from west to east longitude in Fig. 3 are the locations of six, low-to-middle latitude
219 Dobson stations operating in 1978/79—Mauna Loa HI, Tallahassee FL, Natal Brazil, Poona
220 India, Cairns Australia, and Invercargill New Zealand. Dobson/TOMS tropical total ozone
221 values (in DU) are 290/300 (Mauna Loa, HI), 264/272 (Natal), 260/272 (Pune), and 233/256
222 (Cairns). Values at middle latitudes are 300/297 (Tallahassee) and 279/269 (Invercargill). On
223 another day, 15 February, (not shown) the comparison results are—255/269 (Mauna Loa, HI),
224 261/258 (Natal), 256/266 (Pune), 254/255 (Cairns), 287/286 (Tallahassee), and 304/322
225 (Invercargill). There are no clear TOMS/Dobson biases from this set of station comparisons.
226 However, it is also likely that their differing values are a result of the rather loose spatial
227 coincidence criteria (1 day, 2° latitude \times 5° longitude) and/or within the combined error estimates
228 of the TOMS and Dobson data.

229



230 Estimates of SCO are obtained by summing together V6 ozone amounts for the multiple layers
231 from 0.68 hPa to 100 hPa, although fewer profiles extend to 68 and 100 hPa in the tropics. V6
232 Level 3 zonal Fourier coefficients are used for this study because they provide complete data
233 coverage each day (Remsberg and Lingenfelter, 2010). To achieve estimates of SCO, ozone
234 mixing ratios as a function of pressure-altitude are obtained at grid points every 2° latitude and
235 5° longitude from the V6 zonal mean and zonal wave coefficients. The zonal coefficients for 15
236 March are from an archived LIMS directory, day074, in its file named ‘o3_comb_coef.txt’,
237 where the Level 3 pressures have a vertical spacing of six levels per decade of pressure-altitude.
238 Ozone amounts (in DU) are obtained for each pressure layer in the manner of Ziemke et al.
239 (2001, their Appendix B). At low latitudes many of the V6 zonal coefficients at 68 and 100 hPa
240 are often zero for wavenumbers greater than three, indicating that some profile segments were
241 contaminated by cirrus and that their zonal mean values may not be representative. At those
242 levels and latitudes, the lower order wavenumber coefficients are also set to zero, and the zonal
243 mean coefficients are replaced by monthly climatological values from Ziemke et al. (2021) as
244 adjusted to November 1978 based on their Rotated Empirical Orthogonal Function (REOF)
245 values. Figure 4 is a cylindrical map projection of SCO from 64°S to 84°N, generated in the
246 foregoing manner. Largest values are at northern middle and high latitudes, and it is likely that
247 some of that ozone extended southward toward the Equator during wintertime.

248

249 Figure 5 is the V6 TRCO distribution obtained by subtracting the above LIMS column ozone
250 (middle) from TOMS ozone (top). The distribution of TRCO appears somewhat noisy, due to the
251 higher resolution TOMS ozone fields. The three red dots denote Boulder (40°N, 105°W), Lhasa,
252 Tibet (30°N, 91°E), and Santiago, Chile (33°S, 70°W) or where there are decreases in TRCO
253 related, in part, to the effects of orography on TOMS ozone. TRCO in the tropics and southern
254 hemisphere for 15 March is even smaller than the monthly zonal mean for March in Table 1.
255 Notably, TRCO is negative at 70°W from 25°S to 50°S and clearly unphysical. That latitude
256 zone is where V6 temperatures have a zonal mean bias versus MERRA of the order of -0.8 K at
257 both 30 and 50 hPa, which translates to an excess of retrieved V6 ozone of ~14% or ~10 DU in
258 SCO and amounts to an equivalent deficit in zonal mean TRCO. There is also a negative V6
259 temperature bias in the northern subtropics of order -0.6 K but only at 50 hPa, which amounts to



260 biases in SCO and TRCO of no more than 5 DU. But what of the much larger negative TRCO
261 biases at 35°S (70°W and 100°E) and at 40°S (160°W)?

262

263 To the extent that 100 hPa approximates the actual tropical tropopause level, one should be able
264 to obtain reasonable estimates of TRCO versus both longitude and latitude—perhaps to latitudes
265 of ± 30 degrees. Figure 6 shows the distribution of geopotential height for 15 March at the 100-
266 hPa level. Note that there is significant zonal wave activity in the subtropics, or where the SE
267 algorithm used for the generation of Level 3 zonal ozone Fourier coefficients smooths the true
268 amplitudes of the waves. As an example, the Level 3 ozone at 25°S and 46 hPa varies zonally
269 from about 1.6 to 2.0 ppmv, but the RMS agreement between those Level 3 estimates and the co-
270 located Level 2 profile points is no better than 0.3 to 0.4 ppmv. In other words, the maximum
271 and minimum wave amplitudes are underestimated by up to 20%. That wave damping occurs
272 near the peak of the ozone partial pressure profile and contributes significant local biases to
273 SCO. If the zonal waves are nearly stationary, then the reduced wave amplitudes occur over a
274 deeper region of the lower stratosphere, perhaps from 100 to 40 hPa. Reduced zonal wave
275 amplitudes in SCO lead to enhanced zonal variations of TRCO. On the other hand, the effects
276 are due to traveling waves, they are also smoothed because the SE algorithm has a memory of
277 order ± 3 days. As a result, the zonal variations of TRCO are qualitative at best, and the net
278 effects of temperature bias, SE smoothing, and perhaps a small bias in the TOMS ozone can lead
279 to significant errors in TRCO locally.

280

281 Figure 6 shows a weak zonal wave-5 pattern in geopotential at 30 to 40°S that is presumably due
282 to upper tropospheric forcings in that latitude zone. As the tropopause descends to higher
283 pressures at higher latitudes, one may also estimate V6 SCO by extending SCO to lower altitudes
284 using the V6 coefficients for 147 hPa and even 215 hPa, keeping in mind that the accuracy of a
285 V6 ozone profile degrades as its associated V6 temperature profile segment becomes less
286 accurate and imparts a larger bias to retrieved ozone at those levels. For that reason, V6
287 estimates of SCO and associated TRCO distributions are evaluated further only for the tropics
288 and subtropics.



289 **b. 6 May 1979**

290 Figure 7 is the distribution of TOMS ozone for 6 May, and Figure 8 is the associated distribution
291 of V6 SCO. Variations in SCO have a zonal wave-4 structure in the SH subtropics. Figure 9 is
292 the distribution of TRCO, which varies from 0 to -20 DU in the tropics and from 20 to -40 DU in
293 the SH subtropics. Zonal mean temperatures, V6 minus MERRA, are negative at 30 hPa by as
294 much as -1.5 K at 40°S, falling to near zero from 30°S to 15°S, and then becoming positive in
295 the tropics and northern subtropics. Temperature biases at 50 hPa are only slightly negative at
296 SH middle latitudes, increasing to nearly -1.0 K from the SH subtropics to the northern middle
297 latitudes. As for 15 March, temperature bias can explain an underestimate of ~10 DU in TRCO
298 between ±30°. Again, the zonal variations of ozone are smoothed of the order of 20% by the SE
299 algorithm, especially at the 46-hPa level, which affects the zonal amplitudes of SCO and causes
300 the variations of TRCO to be larger than expected. Increasing the wave amplitudes of SCO at
301 30°S, for example, gives to a near uniform zonal distribution of TRCO.

302 **c. 8 November 1978**

303 Figure 10 is the distribution of TOMS ozone for 8 November 1978. Largest total ozone values
304 occur in the southern hemisphere (SH) or in springtime just outside of the polar vortex region.
305 The deep blue area at high latitudes of the northern hemisphere (NH) is in polar night or where
306 TOMS did not observe. TOMS tropical ozone is of the order of 270 Dobson units (DU) and
307 shows a weak wave-1 variation with longitude. Dobson/TOMS total ozone values (in DU) are
308 249/256 (Hawaii), 281/276 (Natal), 244/258 (Poona), and 260/276 (Cairns). Total ozone
309 agreement at middle latitudes is 288/283 (Tallahassee) and 361/363 (Invercargill). Again, there
310 are no clear indications of a bias in TOMS ozone on 8 November. Figure 11 shows the
311 distribution of SCO, and its relative lack of zonal structure at low latitudes indicates that zonal
312 ozone variations are weak at and above the 46-hPa level. As with the TOMS data, the largest
313 SCO values occur at SH middle to high latitudes in November.

314

315 Figure 12 is the distribution of TRCO, and its minimum values are of the order of 20 to 35 DU,
316 consistent with tropospheric values for November from satellite data (Fishman et al., 1990) and
317 from balloon soundings of that era (Ziemke et al., 1998). Again, the red dots denote Boulder,



318 Lhasa, and Santiago, where there may be decreases in TRCO related to the effects of orography
319 in the TOMS data. More notably, there are excesses of TRCO at the latitude of 20°S and at
320 about 0°, 40°E, and at 110°E longitude that may indicate transport of ozone from higher latitudes
321 of the lower stratosphere to the uppermost subtropical troposphere. Figure 13 is the distribution
322 of V6 zonal eddy geopotential height at 100 hPa. To a first approximation, wind vectors are
323 oriented from west to east along the eddy contours at midlatitudes and follow cyclonic and anti-
324 cyclonic curvatures that are in opposite directions around lows and highs in the northern and
325 southern hemispheres. Based on the zonal variations in geopotential in Fig. 13, it appears that
326 the relative maximums of TRCO at 0°, 40°E, and at 110°E in Fig. 12 could be due to
327 equatorward transport of stratospheric ozone to below the 100-hPa level. As a check on that
328 prospect, a new distribution of TRCO is calculated, but based on subtracting SCO from above
329 the 147-hPa level rather than the 100-hPa level. The isolated feature of elevated ozone in Fig. 12
330 at 20°S and 0° longitude is nearly unchanged (see *Supplement*), indicating that it is not a result of
331 equatorward transport in the layer from 100 to 147 hPa. A sequence of daily TRCO distributions
332 is shown in the next section as a way of tracking that feature during November.

333

334 **5 Tropospheric Ozone Distributions during November 1978**

335 October and November are when the effects of biomass burning on ozone occur along the
336 southwest coast of Africa (Fishman et al., 1990). Those months are also when temperature
337 biases and SH medium scale wave activity are weaker in the lower stratosphere, such that the V6
338 TRCO values should be more representative of variations in tropospheric ozone. Is there any
339 evidence in November 1978 that ozone was changing just west of 0° degrees longitude in the SH
340 subtropics and tropics?

341

342 To check about that, SCO is integrated down to the 147-hPa level for eight November days (2, 4,
343 6, 8, 12, 15, 19, and 22). Those daily data are separated by three days on average; some days
344 were skipped because they had one orbit of TOMS data missing. In addition, the results for each
345 day of the sequence are nearly independent, as the memory of the V6 Level 3 SE mapping
346 algorithm is of order three days. The associated TRCO results for each day are averaged over



347 the southern tropics from 20°S to the Equator and then assembled as a Hovmöller diagram
348 (longitude-time) in Figure 14. There is a general zonal wave-1 variation (max of ~70 DU near
349 0°, min of ~30 DU near 180°) in early November 1978 or like that in the monthly TRCO
350 distributions of later decades (see Fishman et al., 1990; Ziemke et al., 1996). There is good
351 continuity over time for the maximum around 0° longitude or southern Africa, and there is a
352 decline from ~70 to only ~45 DU from 2 to 22 November. It is posited that the elevated feature
353 indicates chemical production of ozone lower in the troposphere or downwind of biomass
354 burning activities in Africa and that there was a dispersal of that ozone maximum during
355 November. There is also an absolute minimum in the eastern Pacific and a secondary maximum
356 of ~50 DU near 100°E around 8 November, the latter due perhaps to biomass burning activities
357 in the Indonesia region.

358

359 **6 Conclusions**

360 The findings of this exploratory study indicate that estimates of the zonal variability of tropical
361 to subtropical TRCO from LIMS/TOMS are reasonable for November 1978 but are not as
362 reliable from January through May. V6 SCO values contain residual cirrus effects at times in the
363 tropical lowermost stratosphere. To avoid those effects, climatological monthly zonal mean
364 values were substituted at 68 and 100 hPa, prior to calculating SCO in the tropics. Forward
365 model errors and net negative temperature biases of order -1 to -2 K give rise to V6 ozone values
366 that are too large by ~20% at 30 and 50 hPa in the lower stratosphere, particularly in March and
367 May. When considering the effects of the negative temperature biases, one should adjust SCO
368 downward and TRCO upward by the same amount. The V6 mapping algorithm also smoothed
369 ozone zonal wave amplitudes, leading to underestimates of those variations in SCO and
370 overestimates of TRCO consequently.

371

372 Distributions of TRCO are generated for eight days in November 1978, spaced about three days
373 apart. The daily TRCO distributions of the southern tropics are assembled as a Hovmöller
374 diagram, showing elevated ozone (~70 DU) near 0° longitude that diminishes over time (~45
375 DU). Elevated ozone occurs in and just downwind of a region of seasonal biomass burning



376 activity in West Africa. It is concluded that the subtraction of LIMS SCO values from TOMS
377 total ozone provides reasonably accurate estimates of the spatial variations of tropical
378 tropospheric ozone during November 1978.

379

380 **Data Availability.** LIMS V6, SBUV V8, and TOMS V8.6 data are from the NASA GES DISC
381 data archive at <https://disc.gsfc.nasa.gov/>. Dobson data are from the World Ozone and
382 Ultraviolet Data Center (WOUDC) at <https://woudc.org/data/explore.php>.

383

384

385 **Acknowledgements:** Comparison findings on the LIMS V6 versus MERRA temperature and
386 ozone were first presented by Duncan Fairlie at the Extratropical UT/LS Workshop of October
387 19-22, 2009, in Boulder, CO. Murali Natarajan re-generated the plots of V6 versus MERRA
388 temperatures for 26 January for this study, and he provided code for re-gridding the TOMS data
389 to be compatible with those from the LIMS Level 3 product. Lynn Harvey provided MERRA
390 temperatures for 15 March and 6 May, and she made important comments about the manuscript.
391 EER carried out this work as an Emeritus Langley Associate (ELA) at NASA Langley.

392

393

394

395

396

397

398

399

400



401

402 **References**

403 Fishman, J., and Larsen, J. C., 1987, Distribution of Total Ozone and Stratospheric Ozone in the
404 Tropics: Implications for the Distribution of Tropospheric Ozone, *J. Geophys. Res.*, 92, 6627-
405 6634, <https://doi.org/10.1029/JD092iD06p06627>, 1987.

406

407 Fishman, J., Watson, C. E., Larsen, J. C., and Logan, J. A., Distribution of Tropospheric Ozone
408 Determined from Satellite Data, *J. Geophys. Res.*, 95, no. D4, 3599-3617,
409 <https://doi.org/10.1029/JD095iD04p03599>, 1990.

410

411 Gaudel, A., Bourgeois, I., Li, Meng, Chang, K-L., Ziemke, J., Sauvage, B., Stauffer, R. M.,
412 Thompson, A. M., Kollonige, D. E., Smith, N., Hubert, D., Keppens, A., Cuesta, J., Heue, K-P.,
413 Veeffkind, P., Aikin, K., Peischl, J., Thompson, C. R., Ryerson, T. B., Frost, G. J., McDonald, B.
414 C., and Cooper, O. R.: Tropical Tropospheric Ozone Distribution and Trends from In Situ and
415 Satellite Data, *Atmos. Chem. Phys.*, 24, 9975–10000, <https://doi.org/10.5194/acp-24-9975-2024>,
416 2024.

417

418 Heglin, M. I., Tegtmeier, S., Anderson, J., Bourassa, A. E., Brohede, S., Degenstein, D.,
419 Froidevaux, L., Funke, B., Gille, J., Kasai, Y., Kyrola, E. T., Lumpe, J., Murtagh, D., Neu, J. L.,
420 Perot, K., Remsberg, E. E., Rozanov, A., Toohey, M., Urban, J., von Clarmann, T., Walker, K. A.,
421 Wang, H-J., Arosio, C., Damadeo, R., Fuller, R. A., Lingenfelter, G., McLinden, C., Pendelbury,
422 D., Roth, C., Ryan, N. J., Sioris, C., Smith, L., and Weigel, K.: Overview and update of the
423 SPARC Data Initiative: comparison of stratospheric composition measurements from satellite
424 limb sounders, *Earth Syst. Sci. Data*, 13, 1855-1903, <https://doi.org/10.5194/essd-13-1855-2021>,
425 2021.

426



427 Herman, J. R., Hudson, R., McPeters, R., Stolarski, R., Ahmad, Z., Gu, X.-Y., Taylor, S., and
428 Wellemeyer, C., A new self-calibration method applied to TOMS and SBUV backscattered
429 ultraviolet data to determine long-term global ozone change, *J. Geophys. Res.*, 96 (D4), 7531–
430 7545, <https://doi.org/10.1029/90JD02662>, 1991.

431

432 McPeters, R. D., Heath, D. F., and Bhartia, P. K.: Average ozone profiles for 1979 from the
433 NIMBUS 7 SBUV instrument, *J. Geophys. Res.*, 89, D4, 4967-5380,
434 <https://doi.org/10.1029/JD089iD04p05199>, 1984.

435

436 Remsberg, E. E., Russell III, J. R., Gille, J. C., Gordley, L. L., Bailey, P. L., Planet, W. L., and
437 Harries, J. E.: The validation of Nimbus 7 LIMS measurements of ozone, *J. Geophys. Res.*, 89,
438 <https://doi.org/10.1029/JD089iD04p05161>, 1984.

439

440 Remsberg, E. E., and Wu, C.-Y.: Comparisons of satellite ozone data in the lower stratosphere
441 for 1978/79, *J. Geophys. Res.*, 94, <https://doi.org/10.1029/JD094iD05p06419> , 1989.

442

443 Remsberg, E., Lingenfelter, G., Natarajan, M., Gordley, L., Marshall, B. T., and Thompson, R.
444 E.: On the quality of the Nimbus 7 LIMS version 6 ozone for studies of the middle atmosphere,
445 *J. Quant. Spectros. Rad. Transf.*, 105, no. 3, 492-518, <https://doi.org/10.1016/j.jqsrt.2006.12.005>,
446 2007.

447

448 Remsberg, E., and Lingenfelter, G.: LIMS Version 6 Level 3 dataset, NASA Tech. Memo. 2010-
449 216690, 13 pp., available at
450 https://ntrs.nasa.gov/archive/nasa/casi.ntrs.nasa.gov/20100017330_2010018643.pdf , 2010.



451

452 Remsberg, E., Natarajan, M., Fairlie, T. D., Pawson, S., Wargan, K., Coy, L., Lingenfelser, G.,
453 and Kim, G.: On the inclusion of limb infrared monitor of the stratosphere (LIMS) ozone in a
454 data assimilation system, *J. Geophys. Res.*, 118, 7982-8000, [https://doi.org/10.1002/jgrd.50566-](https://doi.org/10.1002/jgrd.50566-2013)
455 [2013](https://doi.org/10.1002/jgrd.50566-2013), 2013

456

457 Remsberg, E., Harvey, V. L., Krueger, A., and Natarajan, M.: Residual temperature bias effects in
458 stratospheric species distributions from LIMS, *Atmos. Meas. Tech.*, 14, 2185–2199,
459 <https://doi.org/10.5194/amt-14-2185-2021>, 2021.

460

461 Ziemke, J. R., Chandra, S., Thompson, A. M., and McNamara, D. P.: Zonal asymmetries in
462 southern hemisphere column ozone: Implications of biomass burning, *J. Geophys. Res.*, 101,
463 <https://doi.org/10.1029/96JD01057>, 1996.

464

465 Ziemke, J. R., Chandra, S., and Bhartia, P. K.: Two new methods for deriving tropospheric
466 column ozone from TOMS measurements: The assimilated UARS MLS/HALOE and
467 convective-cloud differential techniques, *J. Geophys. Res.*, 103,
468 <https://doi.org/10.1029/98JD01567>, 1998.

469

470 Ziemke, J. R., Chandra, S., and Bhartia, P. K.: "Cloud slicing": A new technique to derive upper
471 tropospheric upper tropospheric ozone from satellite measurements, *J. Geophys. Res.*, 106,
472 <https://doi.org/10.1029/2000JD900768> , 2001.

473

474 Ziemke, J. R., Chandra, S., Duncan, B. N., Froidevaux, L., Bhartia, P. K., Levelt, P. F., and
475 Waters, J. W.: Tropospheric ozone determined from Aura OMI and MLS: Evaluation of



476 measurements and comparison with the Global Modeling Initiative's Chemical Transport Model,
477 J. Geophys. Res., 111, <https://doi.org/10.1029/2006JD007089> , 2006.

478

479 Ziemke, J. R., Labow, G. J., Kramarova, N. A., McPeters, R. D., Bhartia, P. K., Oman, L. D.,
480 Frith, S. M., and Haffner, D. P., A global ozone profile climatology for satellite retrieval
481 algorithms based on Aura MLS measurements and the MERRA-2 GMI simulation, Atmos.
482 Meas. Tech., 14, 6407–6418, <https://doi.org/10.5194/amt-14-6407-2021>, 2021.

483

484

485

486

487

488

489



Table 1--Tropical Tropospheric Column Ozone (TRCO in Dobson units)

Latitude	Nov 78	Dec 78	Jan 79	Feb 79	Mar 79	Apr 79	May 79
30	28	33	44	69	76	76	69
25	26	27	25	48	18	57	53
20	24	20	17	35	19	45	42
15	24	18	15	26	21	35	33
10	27	20	17	21	20	28	28
5	29	25	21	18	22	24	23
0	30	30	27	21	24	22	20
-5	44	36	32	27	23	18	14
-10	44	41	34	30	24	10	8
-15	47	40	32	21	6	1	-3
-20	63	41	31	18	0	-2	-3
-25	66	45	31	20	2	1	-3
-30	73	50	28	16	8	1	1

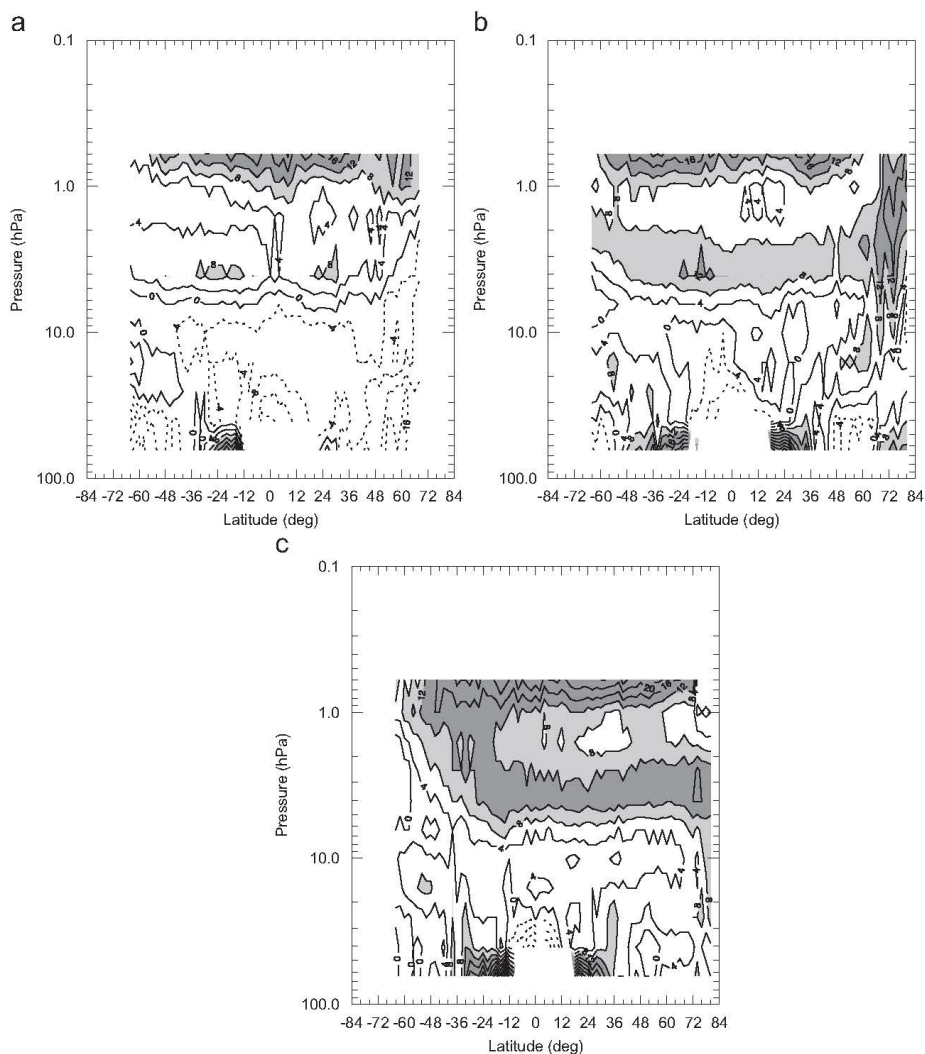
490

491



492 **Figures**

493



494

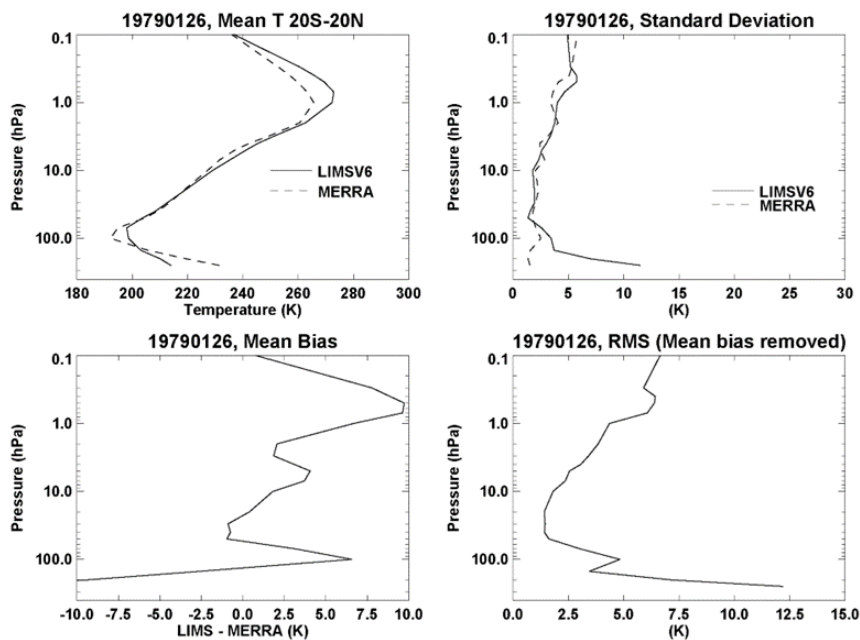
495 Figure 1— Zonal mean cross section of LIMS V6 minus SBUV V8 ozone, divided by SBUV (in
496 %) for (left) 8 November 1978, for (right) 15 March 1979, and for (bottom) 6 May 1979.

497 Contour increment is 4%. Dashed contours are negative and the zero and positive contours are
498 solid. Values greater than +12% are shaded dark; values from +8% to +12% are shaded light.

499



500



501

502 Figure 2—(top left) Zonal mean temperature profiles from LIMS V6 versus MERRA for the
503 latitude band of 20°S to 20°N. (bottom left) Mean bias, V6 minus MERRA, for 26 January
504 1979. (top right) standard deviation about the zonal mean, and (bottom right) RMS deviation
505 with mean bias removed.

506

507

508

509

510

511

512

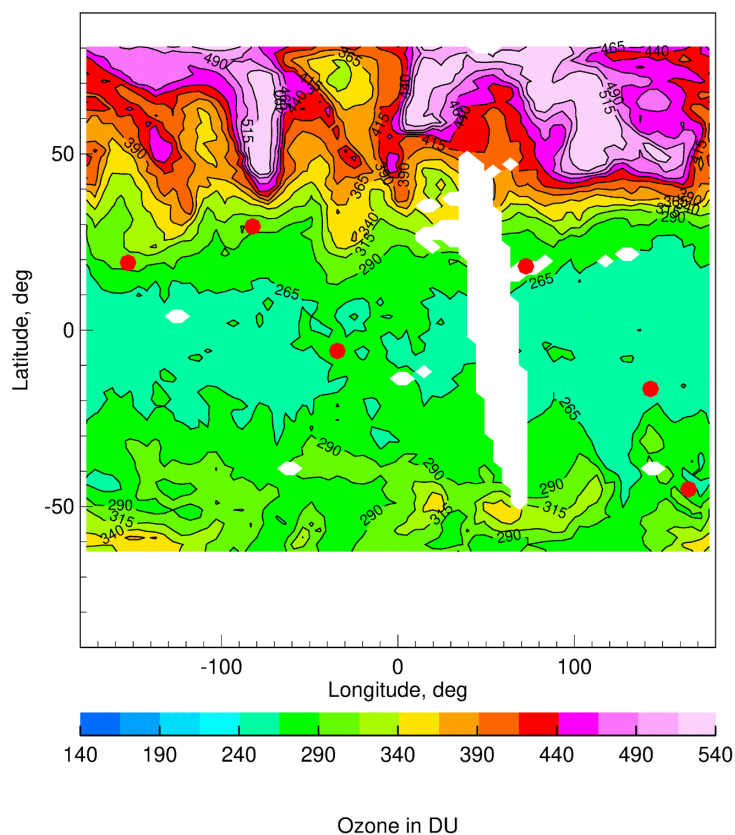
513

514



515

516



517

518 Figure 3—Total ozone distribution in Dobson units (DU) from TOMS data for 64°S to 84°N on
519 15 March 1979. West longitude is negative relative to Greenwich; east is positive. Contour
520 spacing is 25 DU. The white vertical slice near 60°E and other sporadic locations are where
521 TOMS did not operate that day. Red dots are station locations with concurrent Dobson total
522 ozone data.

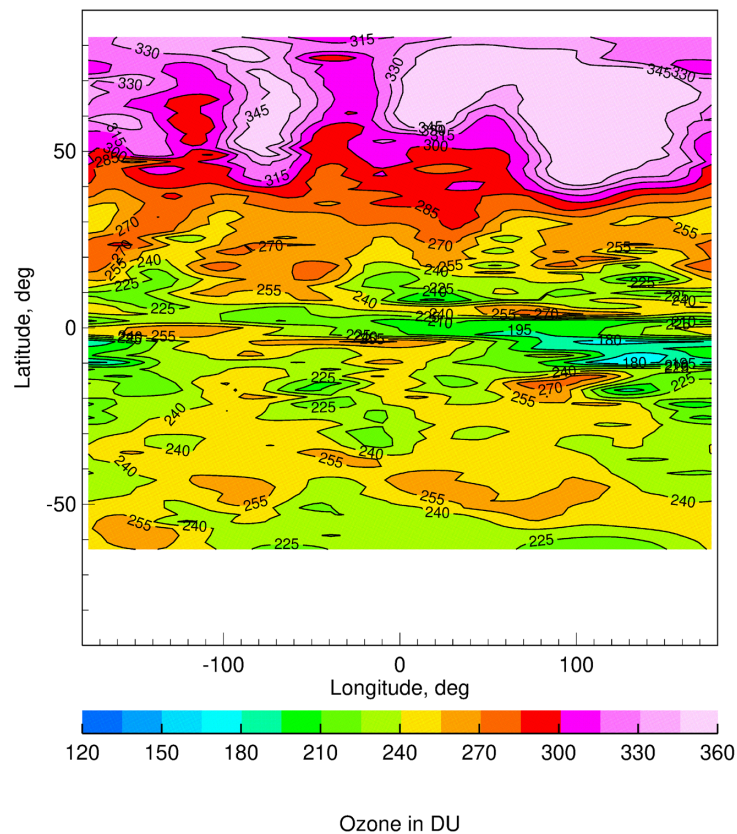
523

524



525

526



527

528 Figure 4—Distribution of SCO (in DU) from LIMS V6 for 15 March; contour spacing is 15 DU.

529

530

531

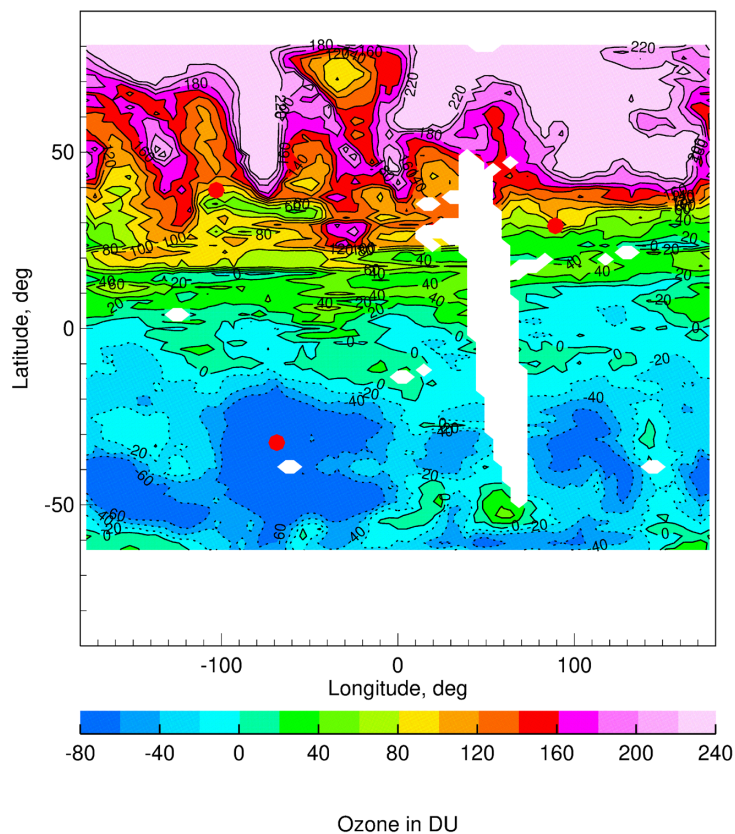
532

533



534

535



536

537 Figure 5—Tropospheric column ozone (TRCO) for 15 March; contour spacing is 20 DU.

538

539

540

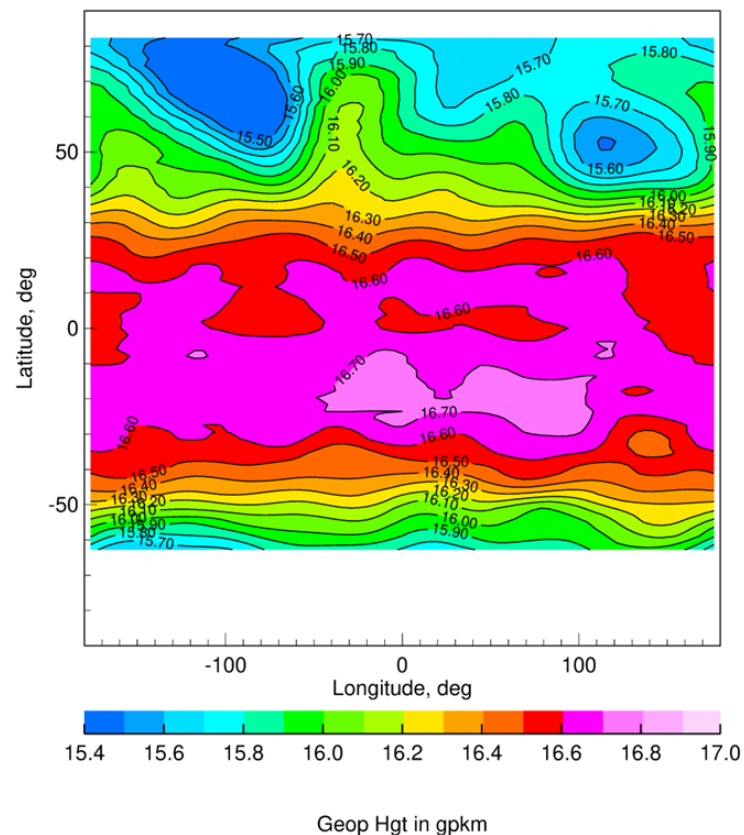
541

542



543

544



545

546 Figure 6— V6 geopotential height contours at 100 hPa for 15 March 1979. Isolines are spaced
547 by 0.1 gpkm.

548

549

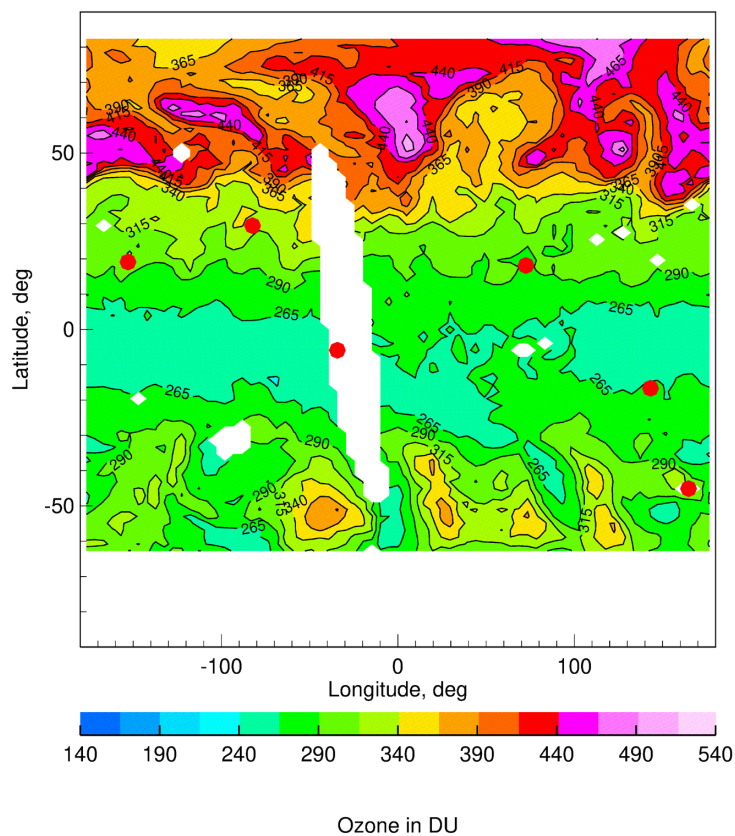
550

551



552

553



554

555 Figure 7—As in Fig. 3, but TOMS data for 6 May 1979. The white vertical slice near 20°W and
556 the small area at 30°, 90°W is where TOMS made no observations that day.

557

558

559

560

561

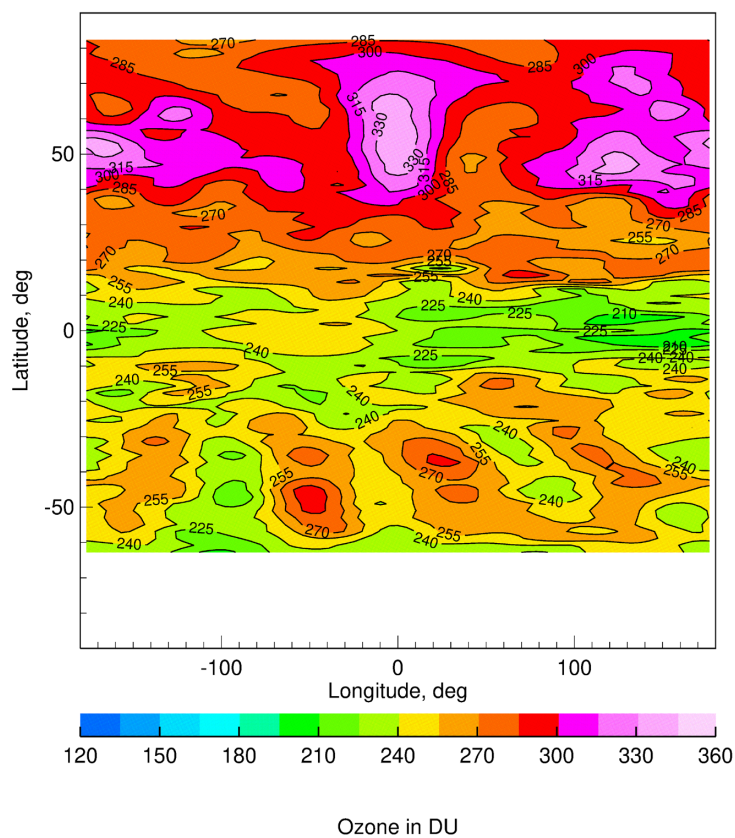
562

563



564

565



566

567 Figure 8—As in Fig. 4, but for SCO on 6 May 1979.

568

569

570

571

572

573

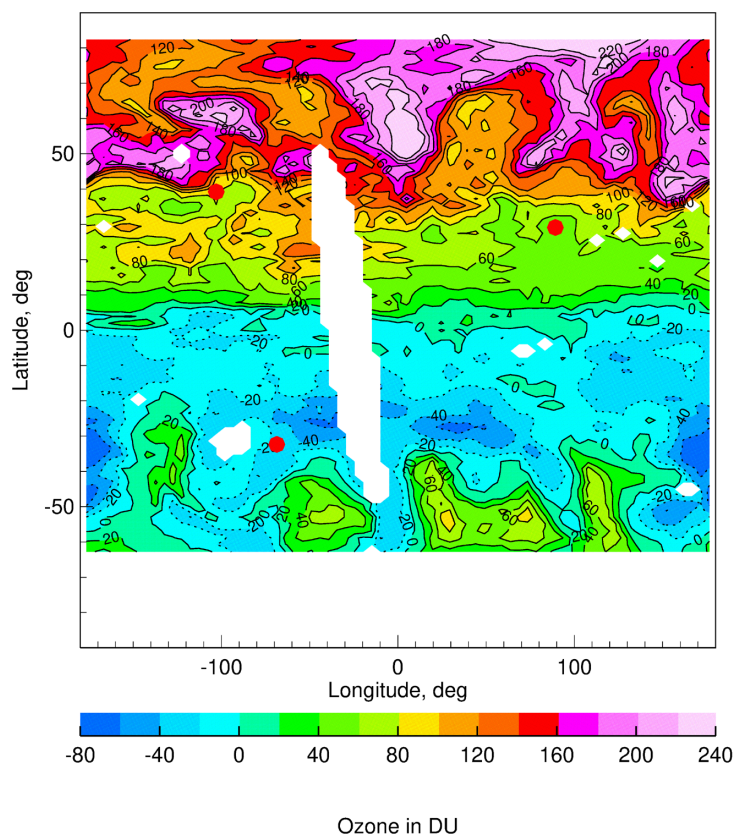
574

575



576

577



578

579 Figure 9—As in Fig. 5, but TRCO for 6 May 1979.

580

581

582

583

584

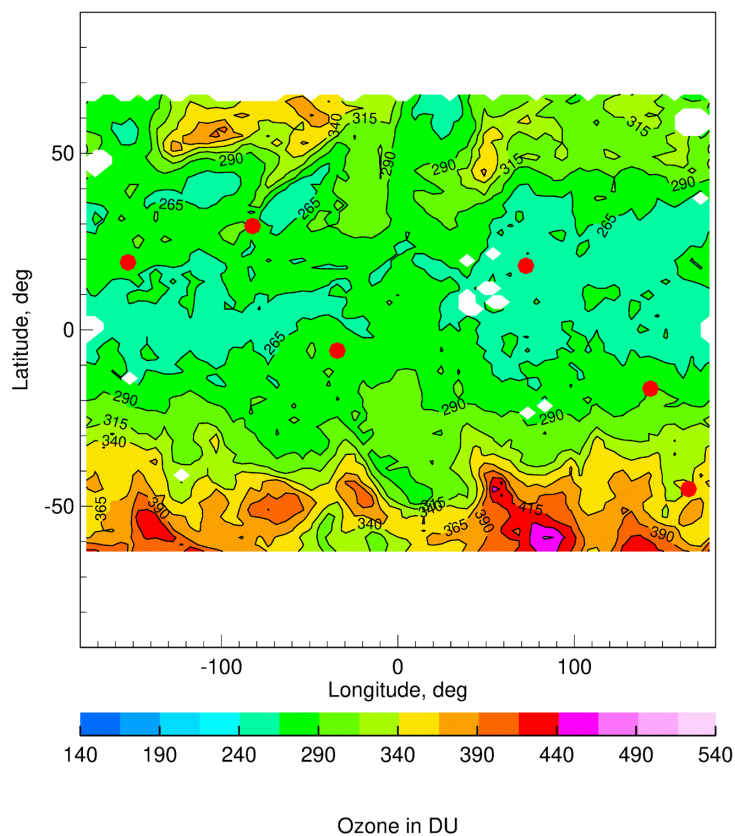
585

586

587



588



589

590 Figure 10—As in Fig. 3, but for TOMS ozone on 8 November 1978.

591

592

593

594

595

596

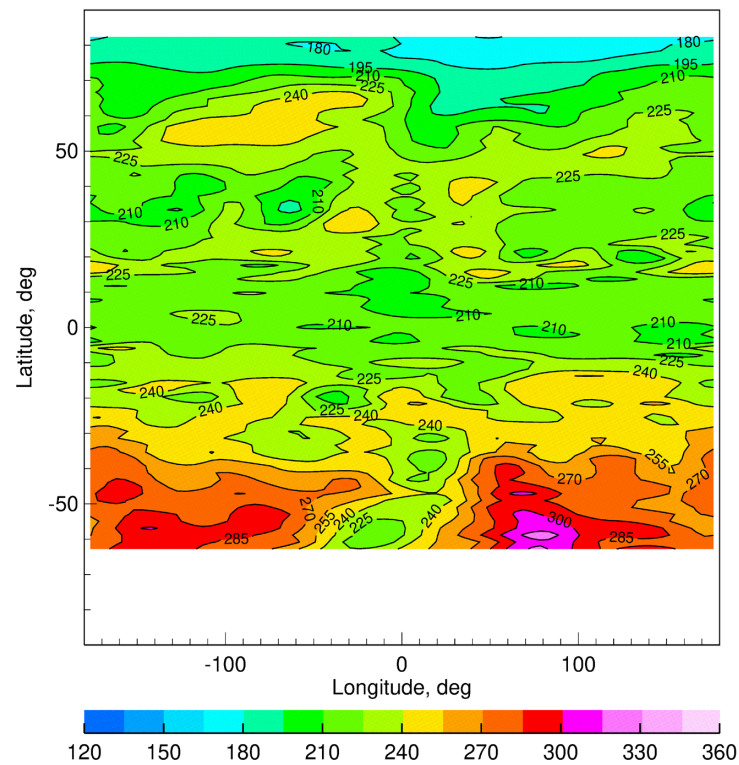
597

598



599

600



Ozone in DU

601

602 Figure 11—As in Fig. 4, but for SCO on 8 November 1978.

603

604

605

606

607

608

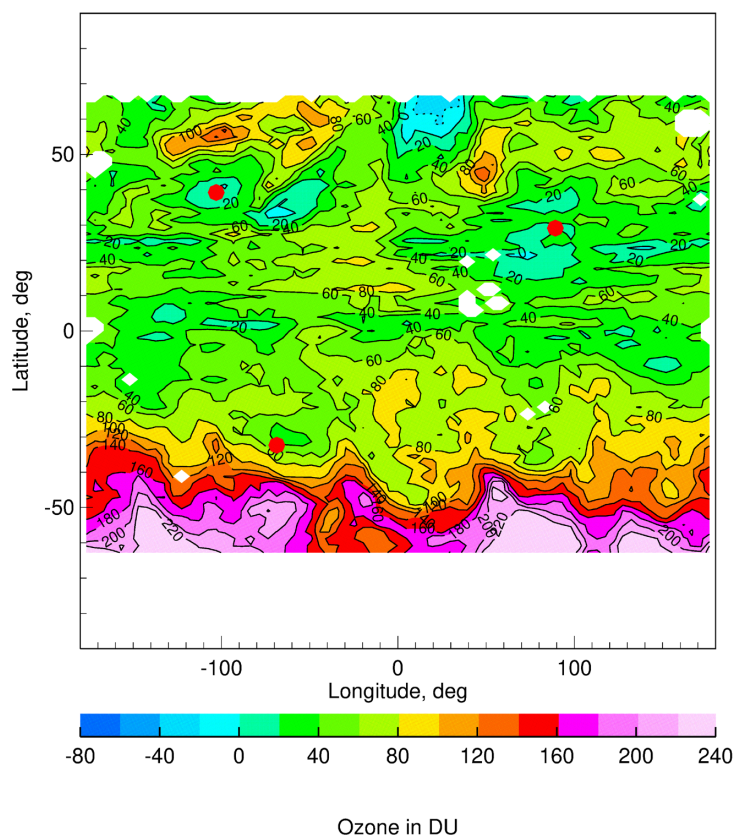
609

610



611

612



613

614 Figure 12—As in Fig. 5, but for TRCO on 8 November 1978.

615

616

617

618

619

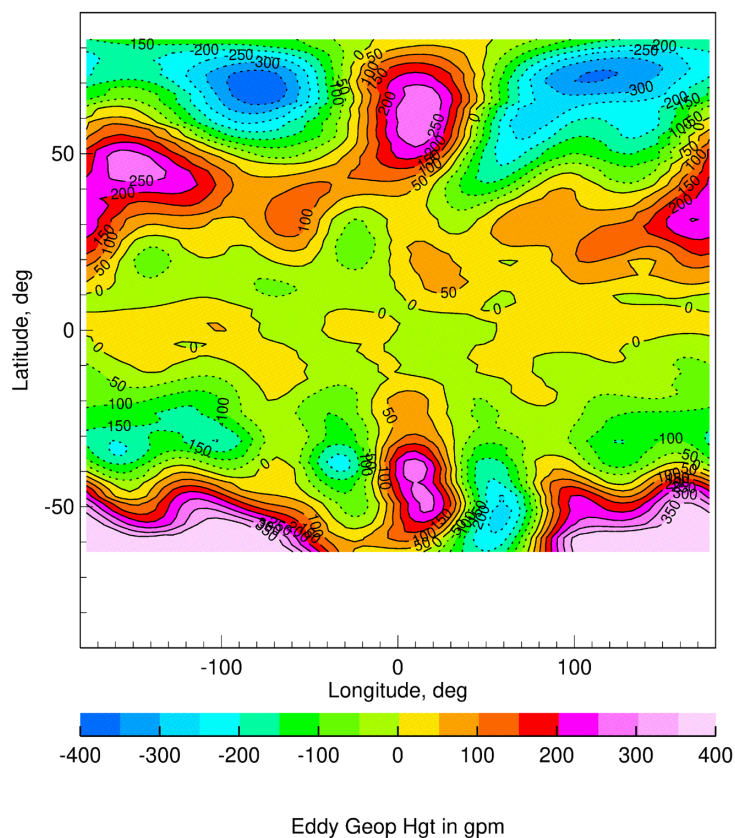
620

621



622

623



624

625 Figure 13—Distribution of zonal eddy geopotential height at 100 hPa on 8 November 1978;

626 contour interval is 50 geopotential meters.

627

628

629

630

631

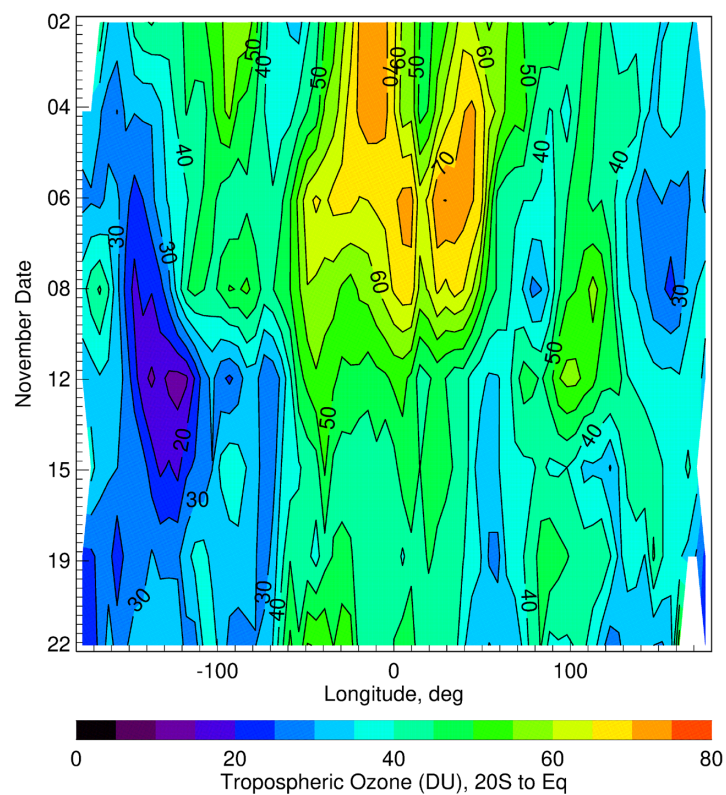
632

633



634

635



636

637 Figure 14—Hovmöller diagram of TRCO results from 2 to 22 November as averaged from 20°S

638 to Equator. Contour interval is 5 DU, and white areas are where TOMS data are missing.

639